Molecular Biology of the Cell
Vol. 11, 3495–3508, October 2000

Bidirectional Translocation of Neurofilaments along Microtubules Mediated in Part by Dynein/Dynactin[V]

Jagesh V. Shah,*†‡ Lisa A. Flanagan,†§ Paul A. Janmey,†‖ and Jean-François Leterrier¶

*Harvard-Massachusetts Institute of Technology Division of Health Sciences and Technology, Cambridge Massachusetts 02139; †Hematology Division, Brigham and Women's Hospital, Harvard Medical School, Boston, Massachusetts 02115; and ¶Unite Mixte de Recherche 6558 Centre National de la Recherche Scientifique, Poitiers University, 86022 Poitiers, France

Submitted April 27, 2000; Revised July 24, 2000; Accepted July 31, 2000
Monitoring Editor: Tim Stearns

Neuronal cytoskeletal elements such as neurofilaments, F-actin, and microtubules are actively translocated by an as yet unidentified mechanism. This report describes a novel interaction between neurofilaments and microtubule motor proteins that mediates the translocation of neurofilaments along microtubules in vitro. Native neurofilaments purified from spinal cord are transported along microtubules at rates of 100-1000 nm/s to both plus and minus ends. This motion requires ATP and is partially inhibited by vanadate, consistent with the activity of neurofilament-bound molecular motors. Motility is in part mediated by the dynein/dynactin motor complex and several kinesin-like proteins. This reconstituted motile system suggests how slow net movement of cytoskeletal polymers may be achieved by alternating activities of fast microtubule motors.

INTRODUCTION

Intermediate filaments (IFs) are 10-nm-diameter filaments that assemble within the cytoplasm of most multicellular organisms. The proteins that comprise IFs are part of a diverse family and are differentially expressed in specialized tissues; vimentin in mesenchymal tissue, desmin in muscle, keratins in epithelium, etc. (reviewed by Fuchs and Weber, 1994). The putative role of IFs in vivo is to maintain cellular, and thereby tissue, integrity under mechanical stress (Galou *et al.*, 1997; Fuchs and Cleveland, 1998). IFs perform this function through unique mechanical properties (Janmey *et al.*, 1991; Leterrier *et al.*, 1996) and interactions with both F-actin (Cary *et al.*, 1994; Yang *et al.*, 1996) and microtubules (Hirokawa *et al.*, 1988; Svitkina *et al.*, 1996; Prahlad *et al.*, 1998; Yang *et al.*, 1999) to form an integrated filament network throughout the cytoplasm (Houseweart and Cleveland, 1998).

Neuronal cells are enriched in specialized IFs, neurofilaments (NFs), which are composed of three subunits, NF-L, M, and H (low, medium, and high based on their electrophoretic mobility). The NF-H and M subunits bear unique carboxy-terminal domains that can link NFs to each other and to other cellular structures, such as microtubules (Hirokawa *et al.*, 1988) and mitochondria (Leterrier *et al.*, 1994). NFs, through their interactions with each other and with other cytoskeletal elements, form a dynamic scaffold that participates in maintaining axonal calibre (Hoffman *et al.*, 1987). This scaffold is constantly renewed much like the cytoskeleton of non-neuronal cells, but the length of neuronal processes presents a barrier to diffusive transport of cytoskeletal proteins. The turnover of the axonal cytoskeleton requires active transport of newly synthesized cytoskeletal proteins from the cell body along the axon. The transport of NF and microtubule (MT) proteins, first documented more than 30 years ago (Weiss and Hiscoe, 1948; Lasek, 1967; Karlsson and Sjostrand, 1968; McEwen and Grafstein, 1968), takes place through an as yet unidentified mechanism (Nixon, 1998) at rates 100 times slower (0.1–1.0 mm/d) than conventional MT motor-driven vesicular cargoes (~50–100 mm/d).

Recent studies have elucidated some elements of the slow transport process through the direct visualization of NF transport in living axons (Wang *et al.*, 2000). In this elegant study a subset of fluorescently tagged NFs was transported down and visualized in the axon of a cultured neuron,

[V] Online version of this article contains video material for Figure 2. Online version is available at www.molbiolcell.org.

‡ Present address: Ludwig Institute for Cancer Research, University of California, San Diego, La Jolla, CA 92093. ‖Present address: Institute for Medicine and Engineering, University of Pennsylvania, Philadelphia, PA 19104.
§ Corresponding author: E-mail address: flanagan@cnd.bwh.harvard.edu.

demonstrating for the first time the saltatory nature of axonal NF transport. The transported NFs exhibited short time-scale motions consistent with a fast anterograde transport velocity interspersed with frequent pauses and short retrograde motions, presumably all combining to result in the net slow velocity measured by traditional pulsed radiolabeling techniques. The visualization of a transported subset of NFs indicates that there exists a pool of NFs bound to molecular motors that contribute to motility.

Here we use a native preparation of neurofilaments to isolate an NF fraction containing NF-bound MT motors. These NF-motor complexes mediate the bidirectional translocation of NFs along MTs in vitro. Biochemical and immunological analyses suggest that dynein and dynactin are in part responsible for the minus end-directed motion of NFs on MTs and that one or a number of kinesin-related proteins make up the plus end component. The biochemical isolation of a functional NF/motor complex represents an essential step in dissecting the molecular components responsible for the slow transport of cytoskeletal elements.

MATERIALS AND METHODS

Purification and Fluorescent Labeling of Native Neurofilaments

Native neurofilaments were prepared from freshly obtained bovine (Arena and Sons, Hopkinton, MA) or rat spinal cords (Institut National de la Santé et de la Recherche Médicale Animal facility, Angers, France) according to Leterrier and Eyer (1987) based on a previous method of Delacourte *et al.* (1980) with modifications (Leterrier *et al.*, 1996). All data presented were obtained with bovine material unless otherwise specified. Spinal cords were homogenized 1:1 (wt:vol) with RB [100 mM 2-(*N*-morpholino)ethanesulfonic acid, 1 mM EGTA, 1 mM $MgCl_2$, pH 6.8]. The spinal cord homogenate was centrifuged at 100,000 × *g* for 1 h at 4°C. The supernatant was collected and incubated with one-half supernatant volume of glycerol at 4°C for 3 h. The glycerol mixture was centrifuged at 150,000 × *g* for one hour at 4°C. The supernatant was decanted and is referred to as "supe" in figures. The pellet was homogenized in a teflon-glass tissue grinder by using RB plus a protease inhibitor cocktail (1 μM leupeptin, 1 μM pepstatin, 0.05 trypsin inhibitor unit (TIU)/ml aprotinin, 0.1 mM chloroquine, 10 nM soybean trypsin inhibitor, 100 μg/ml *N*α-*p*-tosyl-L-arginine methyl ester, and 0.1 mM *N*-tosyl-L-lysine chloromethyl ketone) at 4°C and is referred to as "crude NF" in the figures. The crude NFs were further centrifuged over a two-step sucrose cushion (0.8 and 1.5 M in RB) at 300,000 × *g* for 3 h at 4°C. The supernatant was removed and the pelleted material was gently homogenized in RB with 0.8 M sucrose and protease inhibitors. The homogenized pellet was dialyzed against RB with 0.8 M sucrose and 0.1 mM phenylmethylsulfonyl fluoride for at least 24 h.

NFs were fluorescently labeled by addition of a 40 times molar excess of rhodamine B *N*-hydroxy succinimidyl ester (a kind gift of Dr. Roland Vegners, Latvian Institute for Organic Synthesis, Riga, Latvia) to the crude NFs, incubated for 30 min at 4°C, and subsequently spun over the two-step sucrose cushion to simultaneously purify native NFs and eliminate free dye in the preparation.

Purification, Labeling, and Assembly of Microtubules

Purified tubulin was prepared from bovine brain microtubules and estimated to be ~99% pure as determined by densitometric scanning of Coomassie-stained gels (Vallee, 1986; Malekzadeh-Hemmat *et al.*, 1993). Tubulin was fluorescently labeled with an Oregon Green 488 succinimidyl ester (Molecular Probes, Eugene, OR) according to published protocols (Hyman *et al.*, 1991) or, in the case of rhodamine tubulin, obtained from commercial sources (Cytoskeleton, Boulder, CO). Polarity-marked MTs were grown from brightly fluorescent tubulin polymer seeds in the presence of an *N*-ethylmaleimide-tubulin/unconjugated tubulin mixture (Hyman, 1991). The polymerized tubules were stabilized by the addition of taxol (paclitaxel; Calbiochem, La Jolla, CA) to 10 μM. The ratio of labeled tubulin in polarity-marked tubules varied widely and resulted in a range of apparent MT widths when imaged by fluorescence microscopy, a function of fluorescent intensity, image acquisition times, and image postprocessing (e.g., enlargement).

Motility Assay

NF motility along MTs was observed in flow chambers (~30 μl) prepared from standard microscope slides attached to a coverslip by using double-sided tape (3 M, Minneapolis, MN). The chamber was initially loaded with a dilute solution of polarity marked MTs in RBT buffer (RB + 10 μM taxol). The MTs were allowed to adsorb to the glass surface for 10 min. The chamber was then loaded with 10 μg/ml casein to block the remaining glass surface, preventing nonspecific protein adsorption. The casein solution was flushed out after 10 min with five chamber volumes of RBT buffer. Fluorescently labeled bovine NFs were added to the chamber at 0.1–1 μg/ml. NFs were allowed to incubate with the MTs for at least 30 min. Excess NFs were removed by flushing the chamber with RBT buffer augmented with an oxygen-scavenging antibleaching solution (2 mg/ml glucose, 0.1% β-mercaptoethanol, 360 U/ml catalase, 8 U/ml glucose oxidase) (Kishino and Yanagida, 1988). Biochemical and immunological effectors of motility were preincubated with the NFs for at least 30 min before addition to the motility chamber. Vanadate experiments were carried out at pH 7.5 and without β-mercaptoethanol to prevent vanadate oligomerization and reduction (Penningroth, 1986). These changes did not affect ATP-dependent translocation. Antibody experiments were carried out using an anti-dynein intermediate chain antibody (74.1; Chemicon, Temecula, CA, and 70.1; Sigma, St. Louis, MO), anti-NF antibodies (SMI31, SMI32; Sternberger Monoclonals, Lutherville, MD), an anti-glial fibrillary acidic protein (GFAP) antibody (Sigma) and the corresponding isotype controls (Sigma) used at the same immunoglobulin concentration. All motility assays were carried out at room temperature.

Motility Analysis

Fluorescent filaments were visualized on a Nikon Diaphot 300 inverted microscope equipped with epifluorescence optics and high numerical aperture objectives. Motility was recorded by a silicon-intensified target camera (DAGE-MTI 64L, Michigan, IL) and digitized through a Scion capture card (Scion, Frederick, MD) to a Power PC Macintosh computer (Apple Computer, Cupertino, CA). All video data were captured at 1 frame per second. Trajectory analysis was carried out using NIH-Image (National Institutes of Health, Bethesda, MD) and MATLAB (MathWorks, Natick, MA). Velocity measurements were made on those NFs that showed persistent motion for at least 3 s. Net velocities were calculated by combining all motile events (>40) and calculating the net displacement. Digital colorization was carried out using Adobe Photoshop (Adobe Systems, San Jose, CA). ANOVA analysis was carried out with SPSS (SPSS Inc., Chicago, IL).

Antibodies

Commercial antibodies were obtained for the detection of dynein intermediate chain (70.1; Sigma; 74.1, Chemicon), capZ subunits (α subunit monoclonal 5B12; β subunit monoclonal 3F2; Developmental Studies Hybridoma Bank, Iowa City, IA), NF subunits (SMI31, SMI32; Sternberger Monoclonals), and GFAP (Sigma). Immunoglobulin isotype controls were purchased from Sigma. Dynactin anti-

bodies (anti-p150^{glued}, anti-p50) were kindly provided by K.T. Vaughan (University of Massachusetts Medical Center, Worcester, MA), the anti-HIPYR kinesin peptide antibody was kindly provided by Arshad Desai (Harvard Medical School, Boston, MA), and the conventional kinesin heavy chain antibody, SUK4, was kindly provided by Jonathan Scholey (University of California at Davis, Davis, CA). AS-2 kinesin toxin was provided by Lawrence S. B. Goldstein (University of California at San Diego, La Jolla, CA) through a material transfer agreement. Immunoblots were carried out according to standard methods (Towbin *et al.*, 1979).

NF/Dynein Disruption

NFs (0.04 mg/ml) were incubated with anti-dynein intermediate chain antibody 74.1 (0.02 mg/ml, 1:50 dilution), control antibody (IgG2b, 0.02 mg/ml; Sigma), or no antibody for 1 h at 4°C, and then centrifuged at 100,000 × *g* for 1 h over a 0.8 M sucrose cushion in RB. Pellets were resuspended in SDS-PAGE sample buffer and resolved on 7.5% gels (Laemmli, 1970) and proteins detected by immunoblotting. Protein levels were quantified by scanning densitometry by using NIH-Image software. The antibody signal was normalized to NF content in each lane to determine the amount of dynein intermediate chain that was displaced from the NFs.

NF Detergent Extraction

NFs (0.1 mg/ml) were incubated in RB with 0.4 M sucrose, protease inhibitor cocktail and with 1% Triton X-100, 1 M KCl or buffer for 1 h at 4°C. The mixture was then centrifuged at 100,000 × *g* for 1 h over a 0.8 M sucrose cushion in RB. The two sucrose layers (0.4 and 0.8 M, designated supe and "sucr" in figures) were collected separately as was the pelleted material. A sample of each fraction was resolved by SDS-PAGE and immunoblotted for dynein intermediate chain reactivity (74.1).

Electron Microscopy

Immunoelectron microscopy (immuno-EM) was performed by sequentially incubating glow-discharged, formvar-coated copper grids in the following solutions: RB, buffer A (RB with 2 M glycerol), NFs diluted to 0.05 mg/ml in buffer A, 10 min wash in buffer A, 10 min wash in buffer B (PBS with 1 M glycerol), 30 min in buffer B with 1% goat serum, 30 min in primary antibody diluted into buffer B with 1% goat serum, three 10-min washes in buffer B with 0.1% goat serum, 30 min in secondary antibody (sheep anti-mouse coupled to 8-nm gold particles, kind gift of J.H. Hartwig, Brigham and Women's Hospital, Boston, MA) diluted into buffer B with 1% goat serum, three 10-min washes in buffer B with 0.1% goat serum, 5-min wash in buffer B, and then stained by incubating 1 min in 2% uranyl acetate dissolved in deionized H_2O. Staining of NF and MT-NF mixtures was carried out on glow-discharged, formvar-coated copper grids with 2% uranyl acetate.

For osmium tetroxide-stained sections, NFs in RB + 0.8 M sucrose were mixed with an equal volume of 2% glutaraldehyde in the same buffer. The mixture was incubated for 30 min at room temperature and then spun at low speed, 1000 × *g* for 5 min. The pellet was postfixed with 1% osmium tetroxide in deionized H_2O for 30 min at room temperature. The postfixed pellet was washed twice with deionized H_2O and stained en bloc with 1% uranyl acetate in H_2O for 1h at 4°C in the dark. The pellet was then washed with deionized H_2O twice, and dehydrated using the following protocol: 50% ethanol 45 min, 70% ethanol 45 min, 90% ethanol 45 min, 100% ethanol 45 min repeated twice. Samples were soaked in epoxypropene once, followed by 50% epoxypropene 50% epon before incubation for 10 min and removal of epon by gravitation overnight. Final embedding was in pure epon by polymerization at 37°C for 2 d and 60°C for 2 d. Sections were cut with glass knives by using a Reichert Ultracut and grid mounted sections were poststained with 1% uranyl acetate in deionized water. All samples were observed in a JEOL-1200EX electron microscope at 100 kV.

RESULTS

Natively Purified NFs Contain Primarily NF Triplet Proteins and No Membranous Organelles

NFs were purified in their native polymerized state from mammalian spinal cords according to previously described methods (Delacourte *et al.*, 1980; Leterrier and Eyer, 1987; Leterrier *et al.*, 1996). SDS-PAGE analysis of purified bovine NFs revealed >95% neurofilament protein composed of the three subunits NF-H (200 kDa), NF-M (150 kDa), and NF-L (68 kDa) (Figure 1A). Fluorescent labeling of a rat NF preparation revealed enrichment of the label in the NF triplet proteins (Figure 1B). Osmium tetroxide-stained sections (Figure 1C) and uranyl acetate staining (Figure 1D) of the NF preparation revealed no MT or membranous organelle contamination.

As previously described by Eyer *et al.* (1989), this NF preparation contains significant ATPase activity. The ATPase activity was further characterized to demonstrate a modest (30–40% increase) stimulation by the addition of taxol-stabilized tubulin polymers and sensitivity to micromolar (~10 μM) vanadate and millimolar EDTA (our unpublished results). These data are consistent with the presence of MT-based molecular motors. Furthermore, the inhibition of MT-stimulated ATPase activity at low (10 μM) vanadate concentrations is the biochemical signature of a dynein-like molecular motor.

Natively Purified NFs Are Translocated along MTs

To test the hypothesis that the ATPase activity represents MT motors that have copurified with NFs and that these motors may mediate NF transport, NFs were fluorescently labeled and visualized on MTs fixed to a substrate. Due to their intrinsic flexibility, NFs often appear as compact structures in solution and elongate into filaments when adsorbed to a glass surface (Leterrier *et al.*, 1996). Rhodamine-labeled NFs were introduced into a chamber containing adsorbed fluorescent, taxol stabilized, polarity-marked MTs (Hyman, 1991) at low NF concentrations to permit the visualization of single NFs. After incubation for 30 min, a large fraction of MT contours were decorated with compact NFs.

After the addition of ATP a substantial percentage of the MT-bound NFs (>50%) exhibited bidirectional motion along MTs. Figure 2, A–F (and supplementary information), show representative video sequences of bidirectional NF translocation along MTs. Figure 2, A and B, show examples of an NF with one end bound to the glass surface and the other end stretched and bound to an MT. Here the filamentous nature of the preparation is easily visualized. Figure 2, C–F, show examples of compact NF structures that are deformed by the force provided through the MT motor and in each case, the structure reveals a filamentous component (small arrow). In Figure 2C, the filamentous component appears as a looping structure connecting two previously consolidated NF structures. In Figure 2D, a large NF structure moves predominantly to the plus end of a MT while undergoing a number of shape changes. Figure 2, E and F, both demonstrate the colocalization of the filament along the MT con-

tour, presumably due to opposing forces that stretch out the NFs during translocation. In most cases, the NFs move a significant distance (>4 μm) in a processive manner following MT contours, characteristics that are inconsistent with a diffusive mechanism of motion. Motility was not due to contaminating vesicles because membranous structures were not observed by electron microscopy (Figure 1, C and D) or by inclusion of a fluorescent lipid dye in the motility assay (our unpublished results). In addition, NFs extracted with a nonionic detergent (1% Triton X-100) had qualitatively similar motility characteristics to that of unextracted NFs. Electron micrographs of motility assay samples demonstrated a number of NF-MT electron dense associations that indicate contact points potentially responsible for the motility (Figure 2G).

NF Translocation Is ATP-dependent and Sensitive to Agents That Disrupt MT Motors

To characterize the MT motor(s) involved in the translocation of NFs, the biochemical and immunological sensitivity of the motility was investigated (Figure 3, A–C). Baseline activity was measured as the percentage of MT-bound NFs that translocated along MT contours in the presence of 100 μM Mg^{2+}-ATP. Addition of antibodies specific to NFs resulted in a significant decrease in motile NFs. An antibody to the phosphorylated form of NFs (SMI31) almost completely eliminated the motile behavior, whereas an antibody to the dephosphorylated form (SMI32) did not significantly diminish the motility. The addition of an antibody against glial fibrillary acidic protein, another IF protein present in the spinal cord, did not affect motility. Thus, as suggested above by their filamentous form and purity demonstrated by SDS-PAGE (Figure 1A), the motile elements are largely composed of NF proteins (Figure 3A).

Depletion of ATP by hexokinase and glucose, and chelation of Mg^{2+} by EDTA resulted in a significant decrease in motility, consistent with the presence of ATP-dependent mechanoenzymes (Figure 3B). The addition of vanadate over a broad range of concentrations (5–200 μM) also significantly decreased the motility (Figure 3B). A decrease of motility at low concentrations of vanadate (5–10 μM) is characteristic of a dynein ATPase. Addition of *erythro*-9-(2-hydroxy-3-nonyl)adenine (EHNA), a specific inhibitor of dynein (versus kinesin) ATPase activity (Penningroth, 1986) also decreased NF transport, strongly suggesting a role for dynein in the observed motility. The addition of anti-dynein intermediate chain (DynIC) antibodies 74.1 (Dillman *et al.*, 1996) and 70.1 (Steuer *et al.*, 1990) disrupted NF translocation along MTs to a similar extent as EHNA (Figure 3C). Antibody isotype controls showed similar NF motility to that of ATP alone, demonstrating a specific effect of the anti-dynein intermediate chain antibodies. A kinesin motor toxin, adociasulfate-2 (AS-2), from the Adocia marine sponge (Sakowicz *et al.*, 1998), also disrupted NF motility, indicating a specific role for kinesins in the observed motility.

Figure 3D shows the measured trajectory of representative NFs demonstrating bidirectional motility. The distances traversed by the NFs before changing direction or stopping (up to 4 μm) are consistent with persistent motor driven motion of the NF along the MT in direct contrast to a diffusive mode of motility where the average excursions would be much shorter and ATP-independent (Figure 3B). The analysis of a large number of translocating NFs is summarized in the velocity histogram of Figure 3E. The average velocity in each direction was in the 100–250-nm/s range, consistent with MT motor speeds seen in MT gliding assays (Cohn *et al.*, 1993) and measurements of organelle motility (Vale *et al.*, 1985; Wiemer *et al.*, 1997). Motility in the presence of 100 μM ATP had no significant bias in MT polarity. However, specific disruption of dynein-mediated motility, through EHNA, vanadate (Penningroth, 1986), and the 74.1 DynIC antibody (Leopold *et al.*, 1998), all biased the NF motility toward the plus end (Figure 3F).

Dynein/Dynactin Are Partly Responsible for Minus End-directed Motility

The disruption of NF motility by dynein-specific antibodies directly demonstrates a role for dynein in the translocation visualized. Previous reports of dynein-mediated motility disruption by antibodies has been interpreted as a disruption of dynein–dynactin interactions (Heald *et al.*, 1997; Waterman-Storer *et al.*, 1997). Fractions from the NF purification were probed with antibodies to dynein and members of the dynactin complex. The multiprotein dynactin complex binds dynein and is thought to link the motor to vesicular cargo and regulate its activity (Gill *et al.*, 1991). An antibody to the intermediate chain of dynein shows strong reactivity in the purified NFs (Figure 4A) as does an antibody to the heavy chain (DHC1) of dynein (our unpublished results). The purified NF fraction also contains members of the dynactin complex: $p150^{glued}$ (Figure 4B), p50/dynamitin (Figure 4C) and capZ (Figure 4D). The presence of dynactin complex members in the NF fraction suggests a dynactin-mediated link between NFs and dynein.

The 74.1 DynIC antibody used to block NF motility (Figure 3, C and F) recognizes the same epitope (Leopold *et al.*, 1998) as a previously characterized antibody that displaces dynein intermediate chain from its cargo (Steffen *et al.*, 1997). Incubation of NFs with the 74.1 antibody also displaced DynIC from the NFs (Figure 4E). Similar results were obtained with the 70.1 DynIC antibody (our unpublished results). Normalization of the Western blot signal shown in Figure 4E to total NF content per lane shows that ~50% of the DynIC is released from NFs by the 74.1 antibody, which is consistent with the 50% reduction in motility of NFs observed after treatment with the same antibody (Figures 3C and 4F). In contrast, $p150^{glued}$ was not removed by treatment with the 74.1 antibody, suggesting that members of the dynactin complex remain associated with NFs (Figure 4F). The displacement of DynIC from the NFs by the 74.1 antibody suggests that the disruption of NF motility was the result of decoupling the dynein complex from the NFs, thereby reducing the number of minus end-directed motile events.

To rule out the possibility of a membranous organelle-mediated interaction between NFs and dynein, the NF fraction was treated with a nonionic detergent. The dynein–NF interaction was not disrupted by 1% Triton X-100 (Figure 4G), indicating that the interaction does not involve membranous structures. The interaction between NFs and dynein could, however, be disrupted by 1 M KCl, indicating that the association is labile to high salt treatment (Figure 4G). NFs treated with Triton X-100 had similar motility statistics to control NFs (our unpublished results).

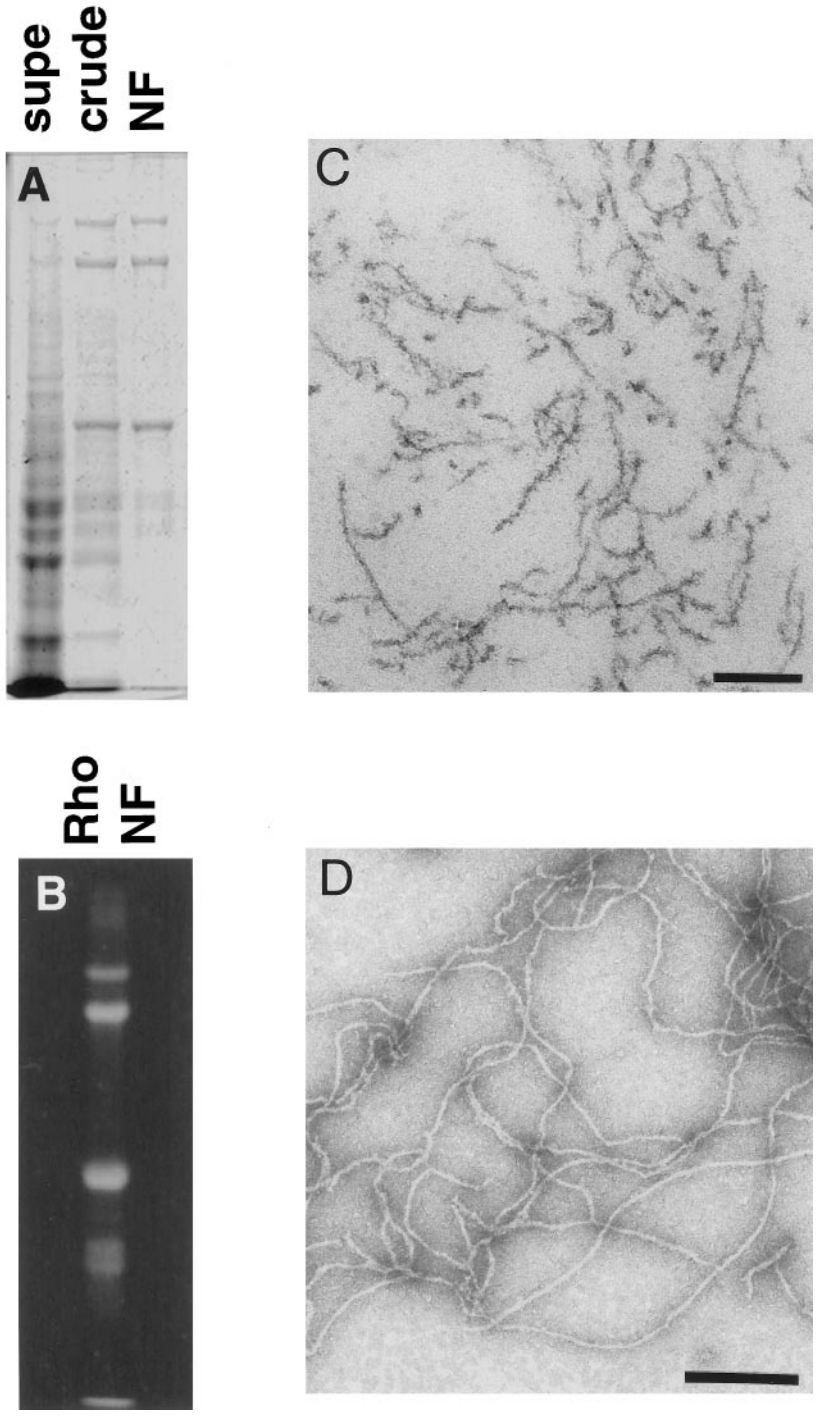

Figure 1. NFs purified from bovine spinal cord have a filamentous structure. (A) SDS-PAGE analysis of a subset of the fractions from the NF purification shows the progressive enrichment of NF triplet protein in the preparation. Supe refers to the supernatant remaining after centrifugation of crude NF, which was further purified over a sucrose cushion to give NF (see MATERIALS AND METHODS). (B) Fluorescent exposure of rhodamine-labeled NF fraction after SDS-PAGE analysis. (C) Electron micrograph of osmium tetroxide-stained sections of pelleted NF fraction. Bar, 200 nm. (D) Electron micrograph of negatively stained NFs from final NF fraction. Bar, 200 nm.

Dynein Is Localized to NFs

NFs were analyzed by immuno-EM to determine dynein localization. NFs were adsorbed to grids, incubated with an anti-DynIC antibody, a gold-conjugated secondary antibody, and negatively stained. Figure 5, A–D, show colocalization of dynein immunoreactivity with NF contours and verify that dynein is not bound to MTs or vesicles. Secondary antibody alone (Figure 5E) or isotype control antibodies (our unpublished results) showed minimal labeling, demonstrating that the dynein immunoreactivity reflects the specific association of dynein with NFs.

The labeling of NFs by anti-DynIC was quantified for comparison to labeling by control antibodies and an antibody to conventional kinesin (SUK4, Figure 5G). The anti-

dynein antibody labeled NFs at a higher density than an isotype-matched immunoglobulin control, secondary antibody only control, or the anti-kinesin antibody, which is consistent with the absence of conventional kinesin reactivity by immunoblotting (Figure 6A). The pattern of dynein labeling on NFs was heterogeneous, with some regions showing dense labeling and other regions sparse labeling. To further quantify this pattern of labeling the density of gold particles along NF segments was measured. This analysis shows that NFs labeled with the secondary antibody control did not contain any segment <250 nm long with more than three beads, whereas the dynein-labeled NFs had many segments that contained anywhere from 4 to 20 beads (Figure 5F). Based on the distribution shown in the histogram the dynein-labeled NFs were separated into those that were densely labeled (≥32 beads/μm) or sparsely labeled (<32 beads/μm). In doing so it was determined that the densely labeled regions contain on average 50 beads/μm, whereas the sparsely labeled regions averaged 1.38 beads/μm (Figure 5G). The densely labeled regions correspond to ~2.7% of the total NF contour length. This result is inconsistent with a random (Poisson) distribution of labeling and shows that the distribution of dynein epitopes along the NFs is heterogeneous.

The density of dynein labeling was compared with the labeling of NFs by a mixture of two antibodies that recognize phosphorylated and nonphosphorylated NF epitopes, SMI31 and SMI32, respectively (Sternberger and Sternberger, 1983). A mixture of these antibodies was used to detect all NFs regardless of phosphorylation state. The density of labeling with the anti-NF antibodies averaged 17.8 beads/μm (Figure 5G). The dense labeling by the anti-dynein antibody is of an even greater density than the labeling by the NF antibodies, possibly due to differences in the affinity of the antibodies or the availability of their epitopes. Taken together, these results show that the labeling of NFs by the anti-dynein antibody is above levels obtained with control antibodies and is heterogeneous, with regions of highly labeled NFs that are at least on the order of staining with NF antibodies. This heterogeneity is also apparent in the motility assay in which a minority of the added NFs bind to and translocate along MTs. Furthermore, this pattern of dynein labeling demonstrates that the binding of dynein to NFs is specific because a nonspecific interaction would result in a sparse, homogeneous, and Poisson-distributed labeling of the NFs with dynein epitopes.

A Number of Kinesin-like Proteins Copurify with NFs

An antibody to the heavy chain of conventional kinesin, SUK4 (Ingold *et al.*, 1988), showed no reactivity in the NF preparation by Western blotting (Figure 6A) or immuno-EM (Figure 5G), although reactivity is observed with intermediate fractions resulting from the NF preparation (Figure 6A). The absence of conventional kinesin, the most prevalent form of kinesin, in the purified NF fraction precludes the possibility of contamination by motor-bound organelles and nonspecific interactions between NFs and soluble kinesins. To identify possible kinesin homologues that may be responsible for the observed plus end-directed motility, an anti-peptide antibody developed against the MT-binding region of *Xenopus* conventional kinesin heavy chain (HIPYR) (Sawin *et al.*, 1992) was used to probe the NF fraction. The anti-HIPYR antibody consistently revealed a number of polypeptides (Figure 6B). The molecular weights of these putative kinesin related proteins were 200, 110, 95, and 85 kDa (lower molecular weight bands were also present with secondary antibody alone and may also represent degradation products). Dephosphorylated NF samples in which NF-H electrophoretic mobility is increased also displayed HIPYR reactivity at 200 kDa, indicating that the 200-kDa band is not NF-H (our unpublished results).

DISCUSSION

The movement of NF proteins in the axon occurs at rates 100 times slower than velocities measured for in vitro molecular motors. Currently, there exists no evidence for a single molecular motor that may be responsible for this process. The data presented here indicate that NFs prepared in their native polymerized state are associated with multiple MT-dependent motors that directly contribute to the bidirectional translocation of NFs along MTs. The motility of NFs along MTs is not diffusive and is ATP-dependent. The minus end-directed component of this motion is partially due to the dynein/dynactin complex, whereas the complement of the motility may be due to multiple kinesin-related proteins found associated with NFs. This bidirectional motion may represent a novel mechanism for slow NF transport.

Transport of NFs in Partially Filamentous Form

Previous work analyzing intracellular IF transport has identified a common theme. In work by Prahlad *et al.* (1998) and Yabe *et al.* (1999), the IF proteins vimentin and NF-M were fused to a green fluorescent protein to monitor their intracellular motion. Both studies indicated that IFs are transported along MT in a compact conformation, referred to as "dots," which later form filamentous structures. It is unknown whether these transported dots consist of IF subunits assembled in IF polymers packed into ball-like aggregates or whether they are unpolymerized IF subunits belonging to multiprotein cargoes associated with molecular motors. The progressive transformation of these transported IF dots into IFs in cells suggests the unraveling of packed polymers (Prahlad *et al.*, 1998; Yabe *et al.*, 1999). The present findings in vitro bring some clues to the possible transition between dot-like IF structures and elongated IF polymers that was observed in vivo by Pralhad *et al.* (1998) and Yabe *et al.* (1999). The NF preparation used in the present work is obtained from adult spinal cord as high-speed–pelleted filaments consisting exclusively of mature phosphorylated polymers (Figure 1, A, C, and D). These filaments can appear in vitro either as compact folded structures or as extended polymers (Figure 2, A–F) because of the high NF flexibility, as previously shown (Leterrier *et al.*, 1996). Such a conformational transition in vitro between ball-like dots and extended IFs is thought to involve ionic interactions of NFs either with charged surfaces or other polymers (Leterrier *et al.*, 1996). A similar transition might thus result in situ from changes in the interactions between the transported IF and other proteins associated with the transport machinery.

Recent studies by Wang *et al.* (2000) have directly visualized extended filament-like NF transport in live cultures

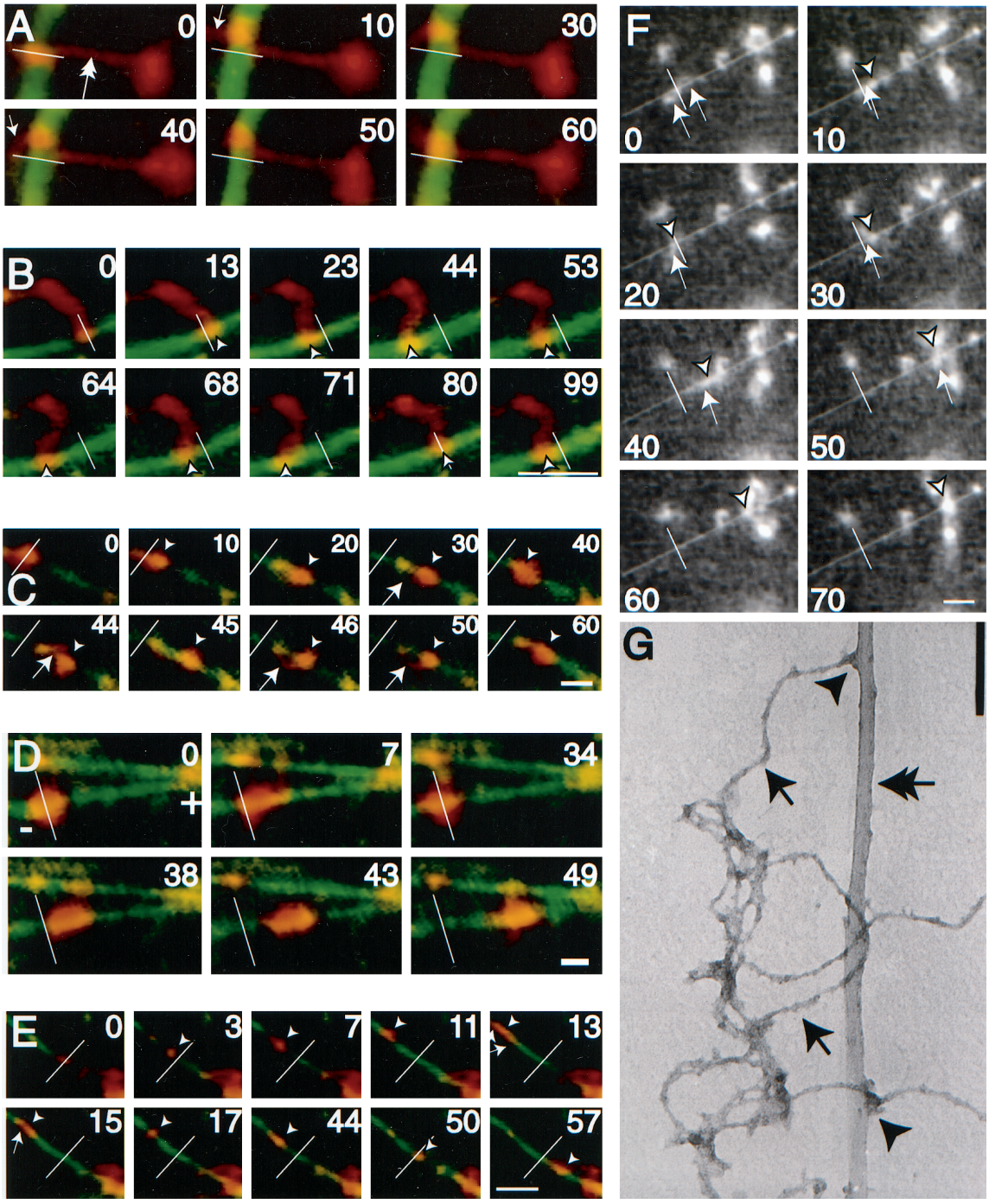

Figure 2. Neurofilaments translocate bidirectionally along microtubules. (A–E) Digitally colorized video sequences of fluorescently labeled NFs (red) translocating along a fluorescently labeled MT (green). White bars represent the position of the NFs at time zero. Arrowheads represent position of the NF on the MT at a particular point in time. In cases where NFs are filamentous the brightest intensity was taken as the position. Arrows indicate filamentous portions of NFs both along the MT (as in E), bound to glass (as in A) or waving in solution (as in C). The outstretched NFs in A (double arrow) and B demonstrate the filamentous nature of the preparation. (F) Uncolorized video sequence of NF translocation along MTs. The white line represents the initial position of the NF and the arrowhead and arrows represent the position of NF and filamentous portions thereof as described above. Bar (A–F), 5 μm. NF motility was carried out in the presence of 100 μM Mg^{2+}-ATP. The plus and minus ends of polarity-marked MTs are indicated in those sequences that use polarity-marked MTs, as are the timings of the video sequences (in seconds). Video sequences corresponding to B, E, and F are available as supplementary information (2b&e.qt.mov and 2f.qt.mov). (G) An electron micrograph of NFs (arrows) and MTs (double arrow) prepared in the same manner as the motility assay demonstrates electron dense MT-NF contacts (arrowheads). Bar, 160 nm.

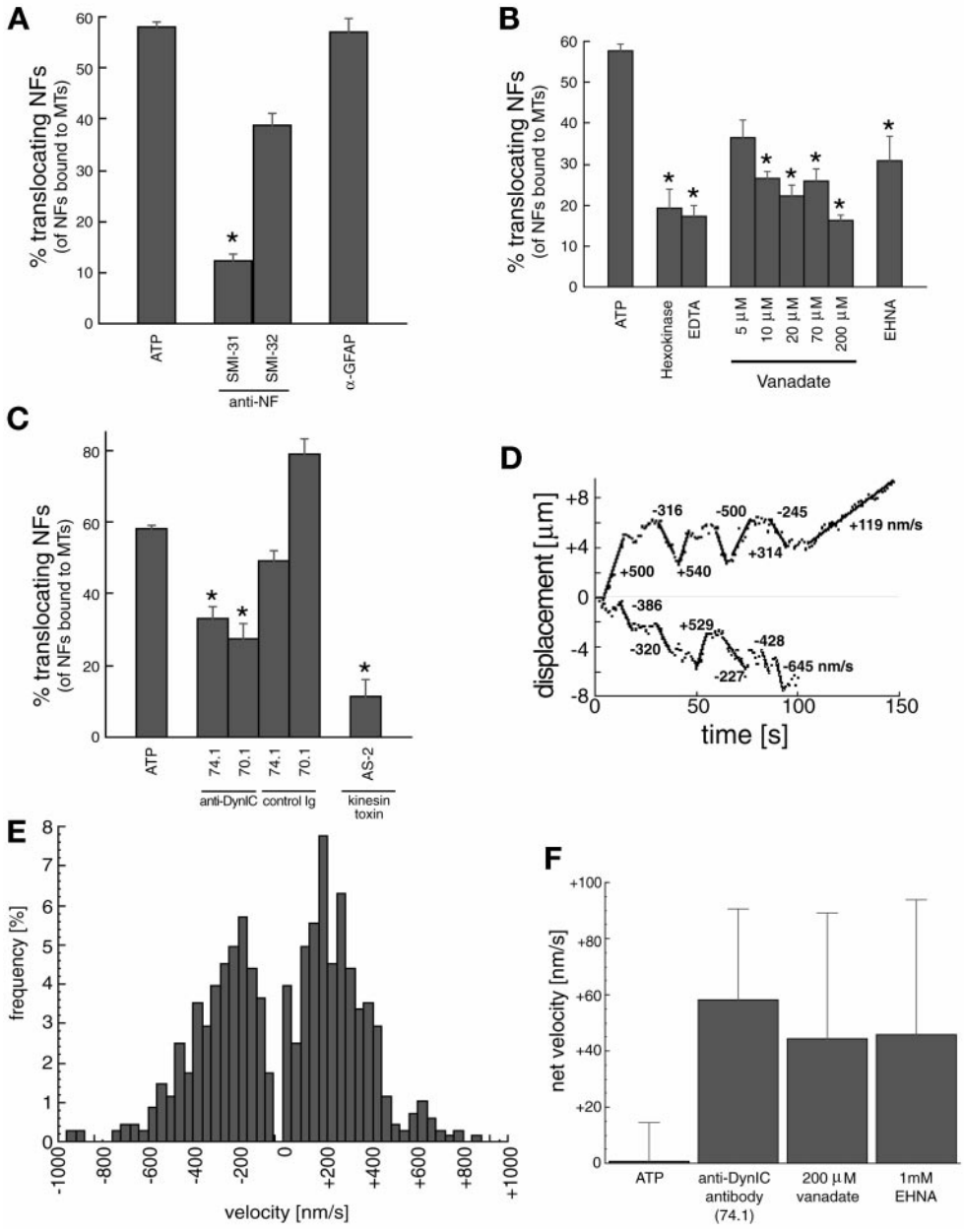

Figure 3. Analysis of neurofilament translocation. (A) Percentage of NFs translocating (of the total bound to MTs) in the presence of 100 μM Mg^{2+}-ATP (baseline) and anti-IF antibodies. SMI31 and SMI32 recognize phosphorylated and nonphosphorylated NF epitopes, respectively. An anti-GFAP antibody is included as a control. Asterisk represents significant change in motility ($p < 0.05$) versus the GFAP control antibody. (B) NF motility is shown in the presence of ATP depletion by 2 U/ml hexokinase/5.5 mM glucose (Hexokinase) and Mg^{2+} depletion by 2 mM EDTA. Vanadate sensitivity for five concentrations (5, 10, 20, 70, 200 μM) and effect of 1 mM EHNA are also shown. Asterisks represent significant change in motility ($p < 0.05$) versus ATP alone. (C) NF transport after preincubation with the two anti-DynIC antibodies 74.1 and 70.1 and the corresponding Ig isotype controls, and a kinesin toxin (AS-2). Asterisks represent significant change in motility ($p < 0.05$) versus the appropriate control Ig (74.1 and 70.1) or ATP (AS-2). The control Ig values were not significantly different than ATP alone ($p > 0.05$). Heights of bars in A–C indicate the average ($\pm$ SEM) of at least 10 independent video sequences comprising at least 150 NFs measured per condition. (D) Trajectories for two representative NFs demonstrate the bidirectional nature of the NF motility. Calculated velocities are shown for various segments of the trajectories. (E) Distribution of velocities of transported NFs in the presence of 100 μM Mg^{2+}-ATP, n = 680 motile events from 90 different NFs. (F) Net velocities (mean $\pm$ SE) of NFs in the presence of dynein inhibitors (74.1 antibody, 200 μM vanadate, and 1 mM EHNA) and under control conditions (100 μM Mg^{2+}-ATP), n > 40 motile events for each condition.

of superior cervical ganglion cells. In this study, the NFs undergo bidirectional motion interspersed with long periods of no motion. The bidirectional motion is consistent with speeds of "fast" transport motors that are comparable to the velocities found in the in vitro system described in this investigation. Specifically, the velocities reported in vitro have slightly lower mean anterograde (0.38 μm/s vs. 0.27 μm/s) and retrograde (0.49 μm/s vs. 0.29 μm/s) velocities than those described by Wang *et al.* (2000). Further evidence that fully polymerized NFs are substrates of in situ active transport is provided by studies in squid giant axons in which injected fluorescent mammalian NFs were transported as large nonmonomeric complexes (Galbraith *et al.*, 1999). However, the hypothesis raised by the present analysis that the in vitro bidirectional motion of fully polymerized mature NF polymers along MTs may reflect the slow transport of NFs in vivo does not exclude the existence of other transport mechanisms of NF subunits in living cells. The transport of NF-M in immature neurons (Pachter and Liem, 1984) and that of ectopically expressed epitope-tagged NF-M in axons of transgenic mice in which most NFs remain in the cell body as a consequence of the expression of a NF-H-LacZ fusion protein (Terada *et al.*, 1996) suggests that NF-M alone can be transported along MTs in a form distinct from the triplet NF heteropolymeric state.

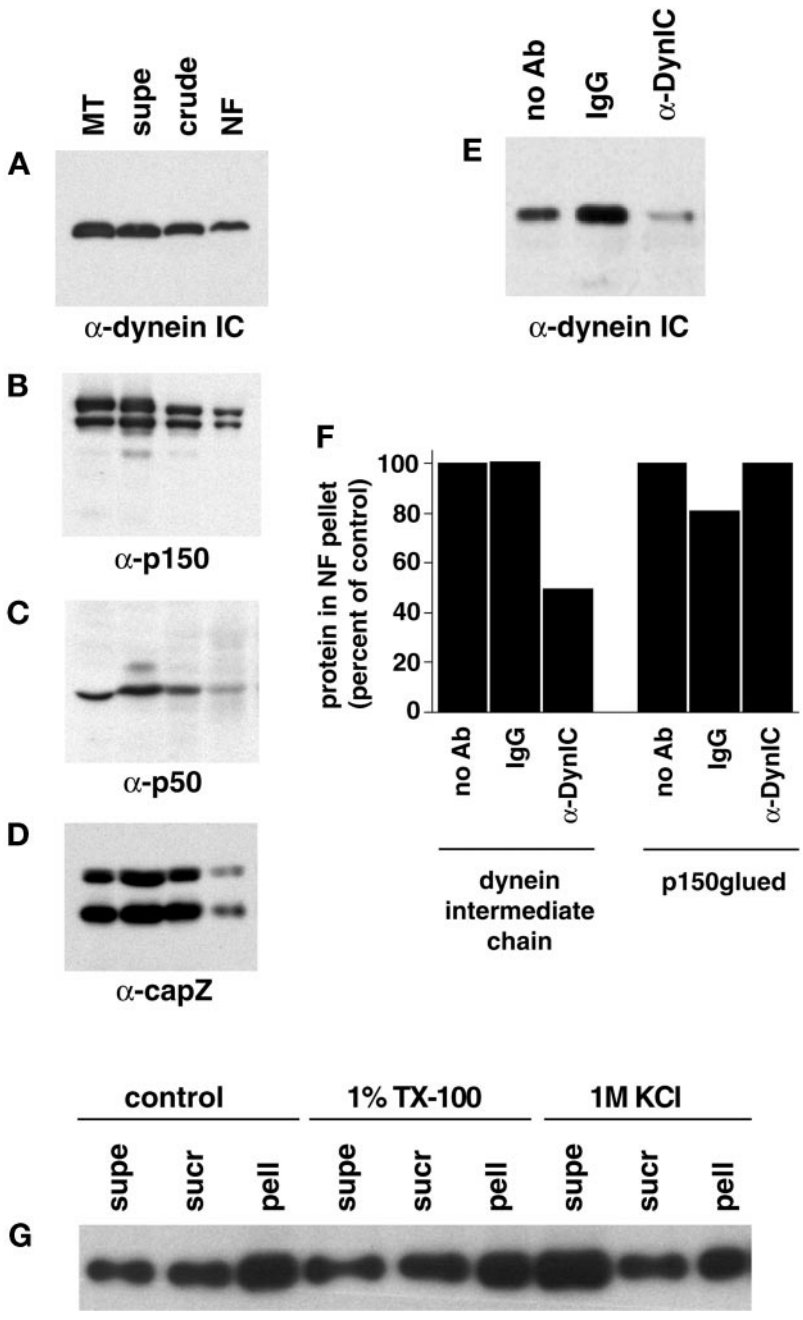

Figure 4. Dynein and dynactin complex members copurify with NFs. Fractions from the NF purification were probed with antibodies to dynein intermediate chain (A), $p150^{glued}$ (showing p150 and the neuronal p135 isoform) (B), p50 (dynamitin) (C), and capZ (α and β subunits) (D). Microtubules prepared from bovine brain were used as a positive control, and the NF fractions are those shown in Figure 1A. Approximately 20 μg of protein was loaded for supe, crude, and NF lanes and ~11 μg for microtubule lanes. (E) The dynein–NF interaction was disrupted with an antibody to the intermediate chain of dynein (74.1) and the NFs pelleted and run on Western blots to determine the amount of dynein that remained bound to NFs. Controls without antibody and with an isotype IgG are shown for comparison. (F) Quantitation of dynein intermediate chain and $p150^{glued}$ immunoreactivity in NF pellets after incubation with the 74.1 dynein intermediate chain antibody, no antibody, or a control IgG. Values were normalized to NF content per lane and are shown as a percentage compared with no antibody controls. (G) NFs were subjected to 1% Triton X-100 (TX-100) or 1 M KCl extraction and pelleted over a sucrose cushion. Equal protein of fractions were separated by SDS-PAGE and probed for dynein intermediate chain immunoreactivity. Supernatant (supe) refers to the fraction above the sucrose cushion, sucrose (sucr) to the sucrose cushion, and pellet (pell) to the pelleted material. A control treatment with no detergent or KCl is also shown.

A Subset of Phosphorylated NFs Translocate along MTs

The disruption of motility by phosphorylation-specific NF antibodies indicated that the translocating NFs are primarily phosphorylated. Furthermore, the heterogeneous labeling of NFs with dynein epitopes indicated that there are at least two populations of NFs, one set with dense motor epitopes and another with sparse or background motor labeling. This type of labeling is inconsistent with nonspecific contamination of the NFs with motors and supports a hypothesis in which small subpopulations of the total phosphorylated NFs form a distinct pool of motile NFs. This finding is consistent with existing data for NF transport in which Jung and Shea (1999) demonstrated the phosphorylation of NFs just before and during NF transport in the murine optic nerve. In addition, in radiolabeling transport studies Nixon and Logvinenko (1986) calculate the transport pool size to be ~70% of radiolabeled NFs, which are themselves a very small fraction of the total axonal NFs, thus the total proportion of motile NFs is expected to be very small. The percentage of purified NFs that label with motor epitopes is also very

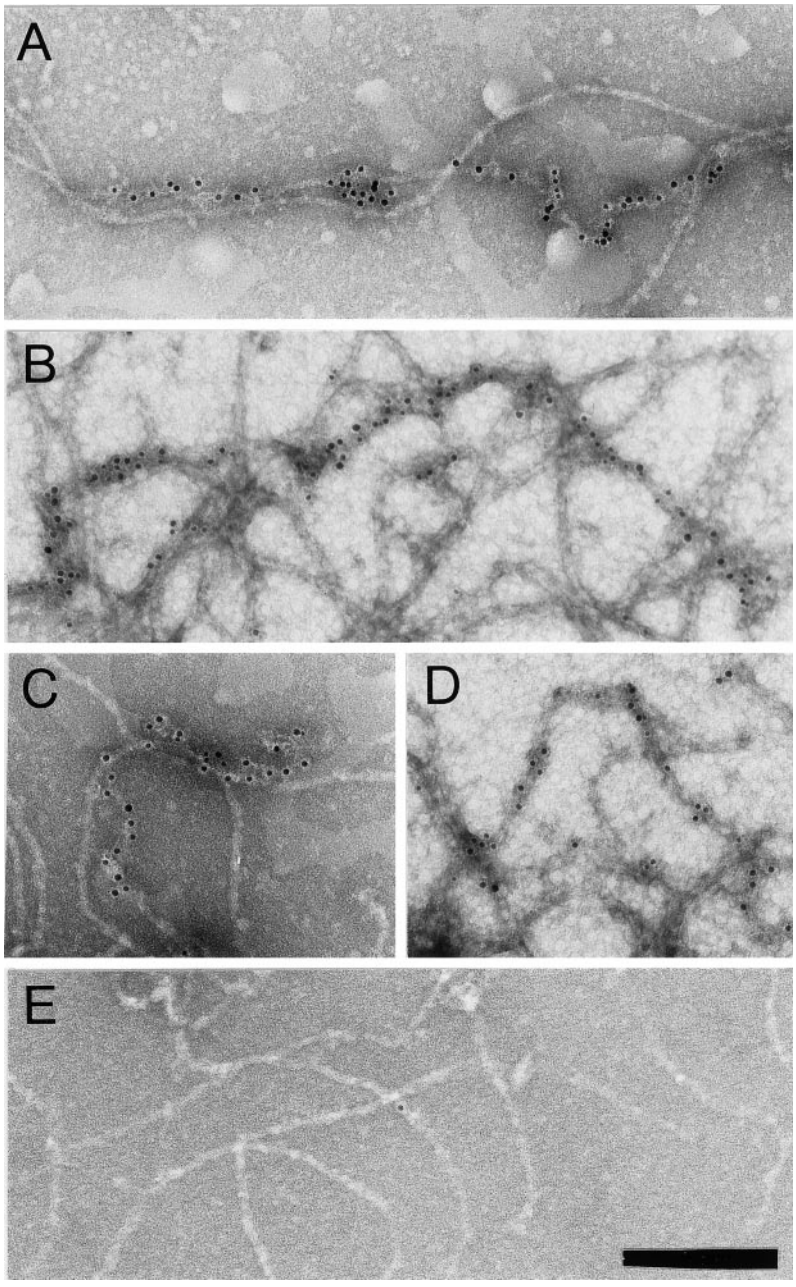

Figure 5. Dynein epitopes localize heterogeneously to NF contours. (A–D) Anti-dynein labeling of NFs shown by Immuno-EM by using anti-DynIC and secondary antibody conjugated to 8-nm gold beads. Anti-dynein antibody labels NFs above background levels and shows a heterogeneous pattern of labeling with areas of particularly dense antibody accumulation. (E) Control electron micrograph of NF treated with secondary antibody alone. Bar (A–E), 200 nm. (F) The number of gold beads was measured along 250-nm segments of NFs from one representative photomicrograph each of anti-dynein labeling and secondary antibody control. The total number of 250-nm segments is as follows: anti-dynein 119 and secondary antibody control 117. (G) The number of gold beads per micrometer of NF is shown for anti-dynein, anti-kinesin (SUK4), an IgG isotype control for the anti-dynein antibody, and a secondary antibody only control. The dynein-labeled NFs were separated into regions that were densely and sparsely labeled (see text). The density of labeling by NF-specific antibodies is included for comparison. The total length of NFs measured for each is as follows: anti-dynein 196.93 μm, anti-kinesin 92.96 μm, IgG control 85.86 μm, secondary only control 147.1 μm, and anti-NF 150.52 μm. The error bars represent the following number of photomicrographs: anti-dynein 5, anti-kinesin 5, IgG control 18, secondary only control 3, and NF 3.

small. Because the data from murine optic nerve (Jung and Shea, 1999) and radiolabeling transport studies (Nixon and Logvinenko, 1986) are from adult animals they would reflect the activity of phosphorylated species of NF, which are similar to the phosphorylated NFs purified from adult animals described in this study. Dephosphorylation of the NFs causes an overall increase in affinity for MTs (our unpublished observations) as previously described by Hisanaga and Hirokawa (1990), making an assessment of motility difficult. However, the dephosphorylation of NFs does not dissociate dynein from NFs (our unpublished observations).

Retrograde Motion of NFs

The association of dynein with NFs partially mediates the minus end-directed motility along NFs. Work by Griffin and colleagues (Glass and Griffin, 1991; Watson *et al.*, 1993) has demonstrated the retrograde flow of NFs in axons, i.e., to the minus end of MTs, by using an in vivo transected nerve model. In these investigations, sciatic nerves from mice with a delayed Wallerian degeneration phenotype were transected and both proximal and distal stumps were monitored for cytoskeletal redistribution. NFs accumulated at both the proximal and distal stumps, demonstrating that retrograde transport of NFs occurs in vivo.

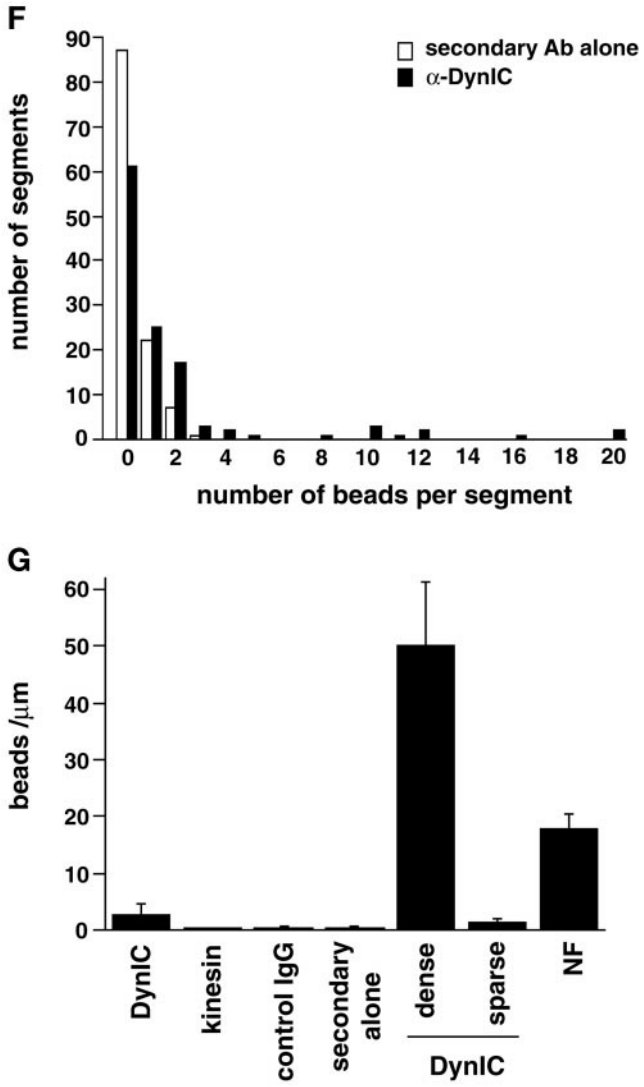

Figure 5 (cont).

Additional evidence for retrograde NF transport is provided by Yabe *et al.* (1999) and Wang *et al.* (2000) who have visualized NF transport in cell culture models. In both studies, a small fraction of the fluorescently tagged NF-containing particles engaged in retrograde motion supporting the presence of a minus end-directed motor.

Together, the retrograde NF motions described in cell culture models and transected nerves indicate that a retrograde component of NF transport functions in vivo. Dynein is one candidate for mediating this retrograde transport of NFs. The present findings demonstrating that proteins of the dynein/dynactin complex are consistently associated with native NFs and are responsible for the minus end component of NF bidirectional motion along MT in vitro support this hypothesis. This NF-bound dynein represents a minor fraction of the main pool of dynein molecules transported in the axon, of which the majority moves with the SCb component (Dillman *et al.*, 1996).

Kinesin-related Proteins Copurify with NFs

The association of intermediate filaments and kinesins has been previously described in a non-neuronal system by Prahlad *et al.* (1998). In spreading cells, a green fluorescent protein-vimentin fusion protein was transported along MTs in packets that later form filaments at the cell periphery. The transport in these cells is mediated by conventional kinesin.

In the neuronal context, Yabe *et al.* (1999) also identify conventional kinesin as an important motor in NF motion in neuroblastoma cells that are actively extending neurites. Yabe *et al.* (1999) demonstrated that microinjection of the SUK4 antibody resulted in cell body accumulation of fluorescently tagged NF subunits. This effect, however, may be an indirect consequence of vesicular cargo accumulation, known to require conventional kinesins.

The disruption of the in vitro NF motility by the kinesin toxin AS-2 provides direct evidence for kinesin-like motor involvement in the observed translocation (Sakowicz *et al.*, 1998). The loss of NF motility in both directions may be due to an effect of AS-2 on dynein itself. The effect of AS-2 on dynein was not investigated in the original description of the toxin (Sakowicz *et al.*, 1998). With a broad-specificity kinesin antibody, anti-HIPYR (Sawin *et al.*, 1992), a set of candidate proteins have been identified each of which may or may not contribute to the motility observed. Of the NF-associated kinesins identified by the HIPYR antibody, the 110-kDa polypeptide detected by the anti-HIPYR antibody does not correspond to the conventional kinesin isoform (kinesin-I) recognized by the SUK4 antibody (Ingold *et al.*, 1988) (Figure 5A). The 110-kDa kinesin-like protein may, however, represent one of the other KIF5/kinesin-I isoforms (Nakagawa *et al.*, 1997) of which two, KIF5A and KIF5C, are restricted to neural tissue. The 85/95 doublet is similar in molecular weight to that of the heterotrimeric kinesin or KIF3/kinesin-II subfamily (Yamazaki *et al.*, 1995), which has been shown to be important in cilia assembly (Nonaka *et al.*, 1998; Marszalek *et al.*, 1999), and is involved in axonal transport (Kondo *et al.*, 1994; Muresan *et al.*, 1998). Finally, the 200-kDa kinesin may represent a member of the KIF1 family of monomeric kinesins that have been previously shown to transport membranous organelles (Okada *et al.*, 1995; Yonekawa *et al.*, 1998).

A Reconstituted System for Slow Axonal NF Transport?

The NFs described here have a number of characteristics that are similar to NFs that are actively transported in axons. As described by many groups, NFs can be transported as filaments (Galbraith *et al.*, 1999; Yabe *et al.*, 1999; Wang *et al.*, 2000) and we have shown here in vitro transport of filamentous NFs along MTs. Jung and Shea (1999) reported that NFs transported down the optic nerve are phosphorylated and antibodies to the phosphorylated form of NF-H and NF-M specifically disrupt NF translocation. Wang *et al.* (2000) demonstrated that NF transport in sympathetic axons is bidirectional and consists of long pauses interspersed by rapid movements in both directions. Although prolonged pausing behavior was not assessed in our study because nonmoving NFs were not chosen for analysis, filaments exhibited bidirec-

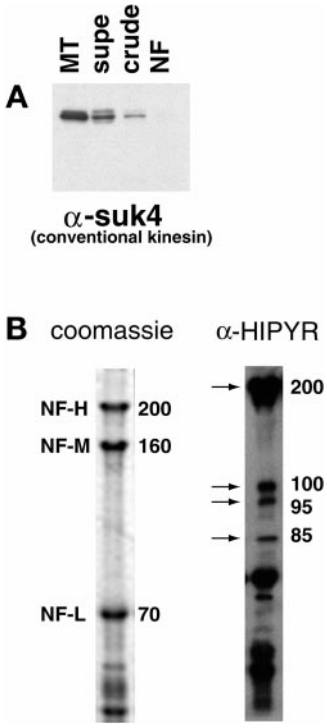

Figure 6. Kinesin-related proteins copurify with NFs. (A) Fractions from the NF purification were probed with the conventional kinesin heavy chain antibody SUK4. (B) The NF fraction was probed with the anti-HIPYR antibody. Arrows mark specific bands detected by the HIPYR antibody. The 200-kDa band does not comigrate with NF-H upon dephosphorylation (increased electrophoretic mobility) and is therefore distinct from NF-H (our unpublished results).

tional motion interrupted by brief pauses. In addition, the retrograde motion is apparently due to the dynein/dynactin complex. Finally, the pattern of motor epitopes seen by immuno-EM demonstrates that only a small subset of filaments has bound motors, as proposed by Nixon and Logvinenko (1986) and that the motors are bound to NFs without an intervening MT. NF transport has been proposed to use binding of NFs to motile MTs (the polymer sliding model of slow transport [Lasek, 1986]) so that NFs need not bind MT motors directly. This study shows that, at least in vitro, NFs can bind MT motors and move along MTs without an intervening motile MT. Further research will be necessary to ascertain whether these two different modes of transport occur in vivo. In conclusion, the in vitro system described here has revealed a number of molecular components that mediate the translocation of NFs along MTs in vitro and may ultimately represent the motors responsible for slow NF transport.

ACKNOWLEDGMENTS

We are grateful to Arshad Desai, Lawrence S.B. Goldstein, John Hartwig, Christoph Schmidt, Kevin Vaughan, and Roland Vegners for reagents; to Manfred Schliwa and Don Cleveland for advice; and to David Bahk and Louise Wang for valuable technical assistance. This work was supported by grants from the National Institutes of Health (P.A.J., L.A.F.), Natural Sciences and Engineering Research Council (J.V.S.), Institut National de la Santé et de la Recherche Médicale (J.F.L.), and North Atlantic Treaty Organization (P.A.J., J.F.L.).

REFERENCES

Cary, R.B., Klymkowsky, M.W., Evans, R.M., Domingo, A., Dent, J.A., and Backhus, L.E. (1994). Vimentin's tail interacts with actin-containing structures in vivo. J. Cell Sci. *107*, 1609–1622.

Cohn, S., Saxton, W.M., Lye, R.J., and Scholey, J.M. (1993). Analyzing microtubule motors in real time. Methods Cell Biol. *39*, 75–88.

Delacourte, A., Filliatreau, G., Boutteau, F., Biserte, G., and Schrevel, J. (1980). Study of the 10-nm-filament fraction isolated during the standard microtubule preparation. Biochem. J. *191*, 543–546.

Dillman, J.F. III, L.P. Dabney, and K.K. Pfister. (1996). Cytoplasmic dynein is associated with slow axonal transport. Proc. Natl. Acad. Sci. USA *93*, 141–144.

Eyer, J., McLean, W.G., and Leterrier, J.F. (1989). Effect of a single dose of β,β'-iminodipropionitrile in vivo on the properties of neurofilaments in vitro: comparison with the effect of iminodipropionitrile added directly to neurofilaments in vitro. J. Neurochem. *52*, 1759–1765.

Fuchs, E., and Cleveland, D.W. (1998). A structural scaffolding of intermediate filaments in health and disease. Science *279*, 514–519.

Fuchs, E., and Weber, K. (1994). Intermediate filaments: structure, dynamics, function, and disease. Annu. Rev. Biochem. *63*, 345–382.

Galbraith, J.A., Reese, T.S., Schlief, M.L., and Gallant, P.E. (1999). Slow transport of unpolymerized tubulin and polymerized neurofilament in the squid giant axon. Proc. Natl. Acad. Sci. USA *96*, 11589–11594.

Galou, M., Gao, J., Humbert, J., Mericskay, M., Li, Z.L., Paulin, D., and Vicart, P. (1997). The importance of intermediate filaments in the adaptation of tissues to mechanical stress: evidence from gene knockout studies. Biol. Cell *89*, 85–97.

Gill, S.R., Schroer, T.A., Szilak, I., Steuer, E.R., Sheetz, M.P., and Cleveland, D.W. (1991). Dynactin, a conserved, ubiquitously expressed component of an activator of vesicle motility mediated by cytoplasmic dynein. J. Cell Biol. *115*, 1639–1650.

Glass, J.D., and Griffin, J.W. (1991). Neurofilament redistribution in transected nerves: evidence for bidirectional transport of neurofilaments. J. Neurosci. *11*, 3146–3154.

Heald, R., Tournebize, R., Habermann, A., Karsenti, E., and Hyman, A. (1997). Spindle assembly in *Xenopus* egg extracts: respective roles of centrosomes and microtubule self-organization. J. Cell Biol. *138*, 615–628.

Hirokawa, N., Hisanaga, S., and Shiomura, Y. (1988). MAP2 is a component of crossbridges between microtubules and neurofilaments in the neuronal cytoskeleton: quick-freeze, deep-etch immunoelectron microscopy and reconstitution studies. J. Neurosci. *8*, 2769–2779.

Hisanaga, S., and Hirokawa, N. (1990). Dephosphorylation-induced interactions of neurofilaments with microtubules. J. Biol. Chem. *265*, 21852–21858.

Hoffman, P.N., Cleveland, D.W., Griffin, J.W., Landes, P.W., Cowan, N.J., and Price, D.L. (1987). Neurofilament gene expres-

sion: a major determinant of axonal caliber. Proc. Natl. Acad. Sci. USA *84*, 3472–3476.

Houseweart, M.K., and Cleveland, D.W. (1998). Intermediate filaments and their associated proteins: multiple dynamic personalities. Curr. Opin. Cell Biol. *10*, 93–101.

Hyman, A.A. (1991). Preparation of marked microtubules for the assay of the polarity of microtubule-based motors by fluorescence. J. Cell Sci. Suppl. *14*, 125–127.

Hyman, A., Drechsel, D., Kellogg, D., Salser, S., Sawin, K., Steffen, P., Wordeman, L., and Mitchison, T. (1991). Preparation of modified tubulins. Methods Enzymol. *196*, 478–485.

Ingold, A.L., Cohn, S.A., and Scholey, J.M. (1988). Inhibition of kinesin-driven microtubule motility by monoclonal antibodies to kinesin heavy chains. J. Cell Biol. *107*, 2657–2667.

Janmey, P.A., Euteneuer, U., Traub, P., and Schliwa, M. (1991). Viscoelastic properties of vimentin compared with other filamentous biopolymer networks. J. Cell Biol. *113*, 155–160.

Jung, C., and Shea, T.B. (1999). Regulation of neurofilament axonal transport by phosphorylation in optic axons in situ. Cell Motil. Cytoskeleton *42*, 230–240.

Karlsson, J., and Sjostrand, O.J. (1968). Transport of labeled proteins in the optic nerve and tract of the rabbit. Brain Res. *11*, 431–439.

Kishino, A., and Yanagida, T. (1988). Force measurements by micromanipulation of a single actin filament by glass needles. Nature *334*, 74–76.

Kondo, S., Sato-Yoshitake, R., Noda, Y., Aizawa, H., Nakata, T., Matsuura, Y., and Hirokawa, N. (1994). KIF3A is a new microtubule-based anterograde motor in the nerve axon. J. Cell Biol. *125*, 1095–10107.

Laemmli, U.K. (1970). Cleavage of structural proteins during the assembly of the head of bacteriophage T4. Nature *227*, 680–685.

Lasek, R.J. (1967). Bidirectional transport of radioactively labeled axoplasmic components. Nature *216*, 1212–1214.

Lasek, R.J. (1986). Polymer sliding in axons. J. Cell Sci. Suppl. *5*, 161–179.

Leopold, P.L., Kreitzer, G., Rempel, S., Pfister, K.K., Rodriguez-Boulan, E., and Crystal, R.G. (1998). Subgroup C adenovirus utilizes microtubules and cytoplasmic dynein during intracellular translocation to the nucleus. Mol. Biol. Cell *9*, 5A.

Leterrier, J.F., and Eyer, J. (1987). Properties of highly viscous gels formed by neurofilaments in vitro. A possible consequence of a specific inter-filament cross-bridging. Biochem. J. *245*, 93–101.

Leterrier, J.F., Kas, J., Hartwig, J., Vegners, R., and Janmey, P.A. (1996). Mechanical effects of neurofilament cross-bridges. Modulation by phosphorylation, lipids, and interactions with F-actin. J. Biol. Chem. *271*, 15687–15694.

Leterrier, J.F., Rusakov, D.A., Nelson, B.D., and Linden, M. (1994). Interactions between brain mitochondria and cytoskeleton: evidence for specialized outer membrane domains involved in the association of cytoskeleton-associated proteins to mitochondria in situ and in vitro. Microsc. Res. Tech. *27*, 233–261.

Malekzadeh-Hemmat, K., Gendry, P., and Launay, J.F. (1993). Rat pancreas kinesin: identification and potential binding to microtubules. Cell. Mol. Biol. *39*, 279–285.

Marszalek, J.R., Ruiz-Lozano, P., Roberts, E., Chien, K.R., and Goldstein, L.S. (1999). Situs inversus and embryonic ciliary morphogenesis defects in mouse mutants lacking the KIF3A subunit of kinesin-II. Proc. Natl. Acad. Sci. USA *96*, 5043–5048.

McEwen, B.S., and Grafstein, B. (1968). Fast and slow components in axonal transport of protein. J. Cell Biol. *38*, 494–508.

Muresan, V., Abramson, T., Lyass, A., Winter, D., Porro, E., Hong, F., Chamberlin, N.L., and Schnapp, B.J. (1998). KIF3C and KIF3A form a novel neuronal heteromeric kinesin that associates with membrane vesicles. Mol. Biol. Cell. *9*, 637–652.

Nakagawa, T., Tanaka, Y., Matsuoka, E., Kondo, S., Okada, Y., Noda, Y., Kanai, Y., and Hirokawa, N. (1997). Identification and classification of 16 new kinesin superfamily (KIF) proteins in mouse genome. Proc. Natl. Acad. Sci. USA *94*, 9654–9659.

Nixon, R.A. (1998). The slow axonal transport of cytoskeletal proteins. Curr. Opin. Cell Biol. *10*, 87–92.

Nixon, R.A., and Logvinenko, K.B. (1986). Multiple fates of newly synthesized neurofilament proteins: evidence for a stationary neurofilament network distributed nonuniformly along axons of retinal ganglion cell neurons. J. Cell Biol. *102*, 647–659.

Nonaka, S., Tanaka, Y., Okada, Y., Takeda, S., Harada, A., Kanai, Y., Kido, M., and Hirokawa, N. (1998). Randomization of left-right asymmetry due to loss of nodal cilia generating leftward flow of extraembryonic fluid in mice lacking KIF3B motor protein. Cell *95*, 829–837.

Okada, Y., Yamazaki, H., Sekine-Aizawa, Y., and Hirokawa, N. (1995). The neuron-specific kinesin superfamily protein KIF1A is a unique monomeric motor for anterograde axonal transport of synaptic vesicle precursors. Cell *81*, 769–780.

Pachter, J.S., and Liem, R.K. (1984). The differential appearance of neurofilament triplet polypeptides in the developing rat optic nerve. Dev. Biol. *103*, 200–210.

Penningroth, S.M. (1986). *erythro*-9-[3-(2-hydroxynonyl)]Adenine and vanadate as probes for microtubule-based cytoskeletal mechanochemistry. Methods Enzymol. *134*, 477–487.

Prahlad, V., Yoon, M., Moir, R.D., Vale, R.D., and Goldman, R.D. (1998). Rapid movements of vimentin on microtubule tracks: kinesin-dependent assembly of intermediate filament networks. J. Cell Biol. *143*, 159–170.

Sakowicz, R., Berdelis, M.S., Ray, K., Blackburn, C.L., Hopmann, C., Faulkner, D.J., and Goldstein, L.S. (1998). A marine natural product inhibitor of kinesin motors. Science *280*, 292–295.

Sawin, K.E., Mitchison, T.J., and Wordeman, L.G. (1992). Evidence for kinesin-related proteins in the mitotic apparatus using peptide antibodies. J. Cell Sci. *101*, 303–313.

Steffen, W., Karki, S., Vaughan, K.T., Vallee, R.B., Holzbaur, E.L.F., Weiss, D.G., and Kuznetsov, S.A. (1997). The involvement of the intermediate chain of cytoplasmic dynein in binding the motor complex to membranous organelles of *Xenopus* oocytes. Mol. Biol. Cell *8*, 2077–2088.

Sternberger, L.A., and Sternberger, N.H. (1983). Monoclonal antibodies distinguish phosphorylated and nonphosphorylated forms of neurofilaments in situ. Proc. Natl. Acad. Sci. *80*, 6126–6130.

Steuer, E.R., Wordeman, L., Schroer, T.A., and Sheetz, M.P. (1990). Localization of cytoplasmic dynein to mitotic spindles and kinetochores. Nature *345*, 266–268.

Svitkina, T.M., Verkhovsky, A.B., and Borisy, G.G. (1996). Plectin sidearms mediate interaction of intermediate filaments with microtubules and other components of the cytoskeleton. J. Cell Biol. *135*, 991–1007.

Terada, S., Nakata, T., Peterson, A.C., and Hirokawa, N. (1996). Visualization of slow axonal transport in vivo. Science *273*, 784–788.

Towbin, H., Staehelin, T., and Gordon, J. (1979). Electrophoretic transfer of proteins from polyacrylamide gels to nitrocellulose

sheets: procedure and some applications. Proc. Natl. Acad. Sci. USA *76*, 4350–4354.

Vale, R.D., Schnapp, B.J., Mitchison, T., Steuer, E., Reese, T.S., and Sheetz, M.P. (1985). Different axoplasmic proteins generate movement in opposite directions along microtubules in vitro. Cell *43*, 623–632.

Vallee, R.B. (1986). Reversible assembly purification of microtubules without assembly-promoting agents and further purification of tubulin, microtubule-associated proteins, and MAP fragments. Methods Enzymol. *134*, 89–104.

Wang, L., Ho, C.L., Sun, D.M., Liem, R.K.H., and Brown, A. (2000). Rapid movement of axonal neurofilaments interrupted by prolonged pauses. Nat. Cell. Biol. *2*, 137–141.

Waterman-Storer, C.M., Karki, S.B., Kuznetsov, S.A., Tabb, J.S., Weiss, D.G., Langford, G.M., and Holzbaur, E.L. (1997). The interaction between cytoplasmic dynein and dynactin is required for fast axonal transport. Proc. Natl. Acad. Sci. USA *94*, 12180–12185.

Watson, D.F., Glass, J.D., and Griffin, J.W. (1993). Redistribution of cytoskeletal proteins in mammalian axons disconnected from their cell bodies. J. Neurosci. *13*, 4354–4360.

Weiss, P.A., and Hiscoe, H.B. (1948). Experiments on the mechanism of nerve growth. J. Exp. Zool. *107*, 315–396.

Wiemer, E.A., Wenzel, T., Deerinck, T.J., Ellisman, M.H., and Subramani, S. (1997). Visualization of the peroxisomal compartment in living mammalian cells: dynamic behavior and association with microtubules. J. Cell Biol. *136*, 71–80.

Yabe, J.T., Pimenta, A., and Shea, T.B. (1999). Kinesin-mediated transport of neurofilament protein oligomers in growing axons. J. Cell Sci. *112*, 3799–3814.

Yamazaki, H., Nakata, T., Okada, Y., and Hirokawa, N. (1995). KIF3A/B: a heterodimeric kinesin superfamily protein that works as a microtubule plus end-directed motor for membrane organelle transport. J. Cell Biol. *130*, 1387–1399.

Yang, Y., Bauer, C., Strasser, G., Wollman, R., Julien, J.P., and Fuchs, E. (1999). Integrators of the cytoskeleton that stabilize microtubules. Cell *98*, 229–238.

Yang, Y., Dowling, J., Yu, Q.C., Kouklis, P., Cleveland, D.W., and Fuchs, E. (1996). An essential cytoskeletal linker protein connecting actin microfilaments to intermediate filaments. Cell *86*, 655–665.

Yonekawa, Y., Harada, A., Okada, Y., Funakoshi, T., Kanai, Y., Takei, Y., Terada, S., Noda, T., and Hirokawa, N. (1998). Defect in synaptic vesicle precursor transport and neuronal cell death in KIF1A motor protein-deficient mice. J. Cell Biol. *141*, 431–441.